EJMI

DOI: 10.14744/ejmi.2018.46330
EJMI 2018;2(3):111–117

Research Article

Additional Findings from Fetal Magnetic Resonance Imaging for Prenatal Sonographic Diagnosis of Central Nervous System Abnormalities

Erdem Yilmaz[1], Baris Bakir[2], Halil Ibrahim Kalelioglu[3], Atil Yuksel[3], Recep Has[3], Burak Tatli[4], Vuslat Lale Bakir[5], Serra Sencer[2]

[1]Department of Radiology, Trakya University Faculty of Medicine, Edirne, Turkey
[2]Department of Radiology, Istanbul University Faculty of Medicine, Istanbul, Turkey
[3]Department of Obstetrics and Gynecology, Istanbul University Faculty of Medicine, Istanbul, Turkey
[4]Department of Pediatrics, Istanbul University Faculty of Medicine, Istanbul, Turkey
[5]Department of Obstetrics and Gynecology, Haseki Training and Research Hospital, Istanbul, Turkey

Abstract

Objectives: The aim of this study was to determine the contribution of fetal magnetic resonance imaging (MRI) in evaluating fetuses with a sonographic diagnosis of a central nerve system (CNS) anomaly.

Methods: Fifty-four fetuses with the sonographic diagnosis of a CNS anomaly underwent fetal MRI. A postnatal brain MRI was performed for 9 infants.

Results: Additional findings were seen with a prenatal MRI in 22 (40%) cases: subependymal nodules (n=2), cortical tubers (n=2), and 1 case each of partial and total agenesis of corpus callosum, pontocerebellar hypoplasia, hypoplastic brain stem, absence of basal ganglia, dysgenetic cerebellum, hyperintensity in the white matter, polymicrogyria, periventricular cyst, thyroglossal duct cyst, partial and total absence of interhemispheric fissure, herniation of inferior cerebellar vermis, arteriovenous fistula, mega cisterna magna, intraventricular hemorrhage, syrinx, and incomplete bony spur in the spinal canal. In all, 18 pregnancies were terminated based on the findings of the prenatal sonography and MRI. The diagnosis was unchanged in 7 cases following postnatal MRI. In 2 infants, additional findings (subependymal tuber and mega cisterna magna) were detected.

Conclusion: Although sonography is an accurate diagnostic modality to evaluate fetuses with CNS anomalies, MRI contributes important additional information, especially regarding the cortical, subependymal, and posterior fossa regions.

Keywords: Fetal anomalies, magnetic resonance imaging, ultrasonography

Ultrasonography (USG) is a valuable imaging technique in fetal examination [1]. The majority of the anomalies detected in the fetus are central nervous system (CNS) anomalies [2]. Multiple gestational anomalies are present in many cases. Therefore, when an anomaly is detected, other possible anomalies should be investigated [3]. However, the detailed description of the anomalies and the detection of concomitant occult anomalies are not always possible due to limitations of USG [4]. Fetal magnetic resonance imaging (MRI) has been shown to contribute to these conditions [5]. The aim of this study was to evaluate the contribution of MRI in patients with CNS anomaly detected by USG.

Methods

Fetal MRI was performed in 56 fetuses (24-36 gestational weeks (mean 30 week) who were diagnosed CNS anomalies with USG during pregnancy between January 2009 and December 2009. The study was approved by the ethics commit-

Address for correspondence: Erdem Yilmaz, MD. Trakya Universitesi Tip Fakultesi, Balkan Yerleskesi, 22030 Edirne, Turkey
Phone: +90 530 404 66 47 **E-mail:** yilmazerdem79@yahoo.com.tr

Submitted Date: September 15, 2018 **Accepted Date:** October 15, 2018 **Available Online Date:** November 15, 2018

Table 1. Sonographic and magnetic resonance imaging findings of fetuses

Fetuses	T	USG Findings	MRI Findings	MRI Additional Findings
1		SPA	(+)	(-)
2		VM, CCA	(+), (+)	(-)
3	+	VM, CCA, SPA	(+), (+), (+)	(-)
4	+	interheminspheric cyst, CCA	(+), (+)	(-)
5		VM, CCA	(+), (+)	(-)
6	+	VM, CCA, SPA	(+), (+), (+)	(-)
7		VM, CCA, SPA	(+), (+), (+)	(-)
8		SPA	(+)	(-)
9	+	CCA	(+)	pontocerebellar hypoplasia
10		VM, SPA	(+), (+)	(-)
11	+	VM, CCA, SPA	(+), (+), (+)	(-)
12		VM, CCA	(+), (+)	(-)
13	+	VM, delayed sulcation, ventricule wall echogenicity	(+), (+), (-)	(-)
14		VM, ventricule wall echogenicity, calcification	(+), (-), (-)	polymicrogyria
15	+	holoprosencephaly, cleft palate, arinia	(+), (+), (+)	thyroglossal duct cyst
16		holoprosencephaly	(+)	abscence of anterior interhemipheric fissure
17		holoprosencephaly, talamic fusion, microcephaly	(+), (+), (+)	abscence of total interheminspheric fissure
18		Vermis anomaly, delayed sulcation, microcephaly	(+), (+), (+)	(-)
19		vermis anomaly, VM	(+), (+), (+)	MCM
20	+	DWM, SPA	(+), (+)	(-)
21		inferior vermis hypoplasia	(+)	periventricular cyst
22		inferior vermis hypoplasia	(+)	(-)
23		inferior vermis hypoplasia	(+)	(-)
24		VM, inferior vermis hypoplasia	(+), (+)	(-)
25		inferior vermis hypoplasia	(+)	(-)
26		inferior vermis hypoplasia	(+)	(-)
27		MSM	(+)	(-)
28		vermis hypoplasia	(+)	(-)
29		MSM	(+)	(-)
30		MSM, gastroschisis	(+), (+)	(-)
31		VM, supratentorial arachnoid cyst	(+), (-)	CCA
32	+	VM, MSM	(+), (+), (+)	dysgenetic cerebellum
33		CCA, SPA, ventriculer synechiae	(+), (+), (+)	absence of basal ganglia
34		VM, dismorphic cerebellum, SPA	(+), (-), (+)	CCA
35	+	SPA, cerebellar hypoplasia	(+), (+)	(-)
36		cardiac rhabdomyoma		cortical tuber
37		cardiac rhabdomyoma		(-)
38		cardiac rhabdomyoma, tuber	(+)	subependymal nodules
39	+	cardiac rhabdomyoma		cortical tuber
40		VM, intraventricular hemorrhage	(+), (+)	(-)
41		inferior vermis hypoplasia, intraventricular hemorrhage	(+), (-)	(-)
42	+	VM, intraventricular hemorrhage	(+), (+)	(-)
43	+	VM, intraventricular hemorrhage	(+), (+)	subependymal nodule
44	+	VM, ventricule wall echogenicity, intraventricular hemorrhage	(+), (-), (+)	hypoplastic brainstem
45	+	VM, parenchymal brain injury, porensefalik kistler	(+), (+), (+)	intraventricular hemorrhage
46		VM, thinning in cerebral parenchyma	(+), (+)	arteriovenous fistula
47		VM, intraventricular hemorrhage	(+), (-)	(-)
48		diastometamyelia	(+)	syrinx
49	+	spina bifida, obliterated cisterna magna	(+), (+)	incomplete bony spur
50		VM, ventricule wall echogenicity, interheminspheric cyst	(+), (-), (+)	(-)

Table 1. Cont.

51		VM, choroid plexus cyst	(+), (-)	inferior vermis herniation
52		VM	(+)	white matter hyperintensity
53		VM, interheminspheric cyst	(+), (-)	(-)
54		IUGR	(+)	(-)
55	+	choroid plexus cyst, polymicrogyria	(+), (+)	(-)
56	+	VM, ventricule wall echogenicity, delayed sulcation	(+), (-), (+)	(-)

T-termination of pregnancy, USG-ultrasonosgraphy, MRI-magnetic resonace imaging, SPA-septum pellicidum agenesis, VM-ventriculomegaly, CCA-corpus callozum agenesis, MCM-Mega cisterna magna, DWM-Dandy Walker malformation, IUGR-intrauterin growth restriction.

tee of our hospital. Prenatal USG examination was performed by three obstetricians (HIK, AY, RH). Fetal MRI examination was performed by three radiologists (EY, BB, SS). MRI evaluation was performed with the knowledge of CNS anomalies.

MRI examination was performed successfully in all patients. MRI examination was performed with 1.5 Tesla MR (Symphony Maestro; Siemens MEdical Systems, Erlangen, Germany) within a week after USG examination. Flexible body coil was used in the examination. MRI examination was performed in the lateral decubitis position in the patients who could not tolerate the supine position. MRI was performed while patients' head was outside of the MRI tube in expectaiton of claustrophobia. No contrast material was given to the patients due to possible teratogenic effects.

Axial, sagittal and coronal T2-weighted HASTE sequences (TE: 91msec, TR: 1200msec, 192x256 matrix, slice tihckness: 3mm, FOV: 207x100 cm, and refocusing flip angle:150), and axial T1 FLASH sequence (TE: 4msec, TR: 199msec, slice thickness: 4mm, FOV: 300x75cm, matrix: 134x256, and flip angle: 70) were performed. T1 FLASH sequences were added to the brain in sagittal and coronal planes in patients with suspected parenchymal and ventricular hemorrhage and in cases with a possible parenchymal lesion. In both sequences, the examination was conducted by holding breath and a sequence lasted 20-25 seconds. The total examination time lasted in 20-30 minutes. Categorical data were expressed with frequency and percentage using SPSS 16.0 for Windows program.

Results

The most common finding was ventriculomegaly (VM) (n=26) in USG. Other common findings were septum pellisidum agenesis (n=10), corpus callosum agenesis (CCA) (n=9), vermis anomaly (n=10), intraventricular hemorrhage (n=6), mega cisterna magna (n=4), and suspicion of cerebral tuber and subependimal nodüle in rhabdomyoma patients (n=4) (Table 1).

In our study, 22 (40%) of 54 patients had additional findings with MRI. Additional findings were subependymal nodules (n=2), cortical tubers (n=2), and one case each of partial and total agenesis of corpus callosum, pontocerebellar hypoplasia, hypoplastic brain stem, absence of basal ganglia, disgenetic cerebellum, hyperintensity in white matter, polimicrogyria, periventricular cyst, thyroglossal duct cyst, partial and total absence of interheminspheric fissure, herniation of cerebella inferior vermis, arteriovenous fistula, mega cisterna magna, intraventircular hemorrhage, syrinx, and incomplete bony spur in the spinal canal.

Ventriculomegaly was also seen in MRI in all fetuses with VM (n=26) (Fig. 1). Fetuses with CCA (n=9) were also seen in MRI. Additional findings of pontocerebellar hypoplasia in a patient with CCA were seen in MRI (Fig. 2). All fetuses with septum pellisidum agenesis (n=10) were also seen in MRI (Fig. 3).

In the cases of holoprosencephaly (n=3), subgroups were identified in MRI. Semilobar holoprosencephaly (n=1) was demonstrated by showing the absence of anterior interheminsferic fissure, and the diagnosis of alobar holoprosencephaly (n=1) was made by showing the absence of total interheminsferic fissure. In 1 of the cases with semilobar holoprosencephaly, thyroglossal duct cyst was shown as additional finding (Fig. 4). Subependymal nodule (n=2), and cortical tubers (n=2) were shown as additional findings in MRI in fetuses that have cardiac rhabdomyoma (Fig. 5).

Intraventricular hemorrhage was detected in 6 cases in USG. However, intraventricular hemorrhage was not ob-

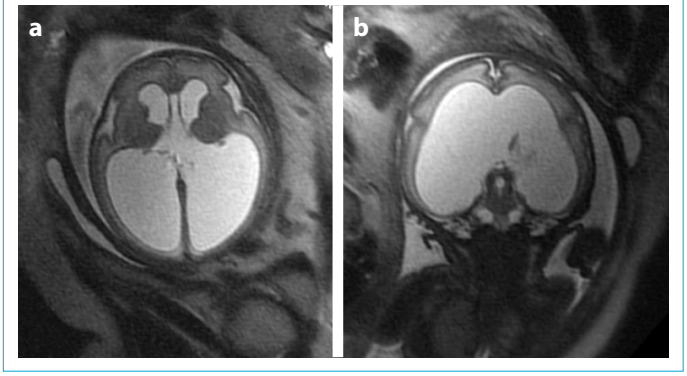

Figure 1 (a, b). Axial **(a)** and coronal **(b)** T2-weighted MRI show significant dilataiton of the lateral ventricles.

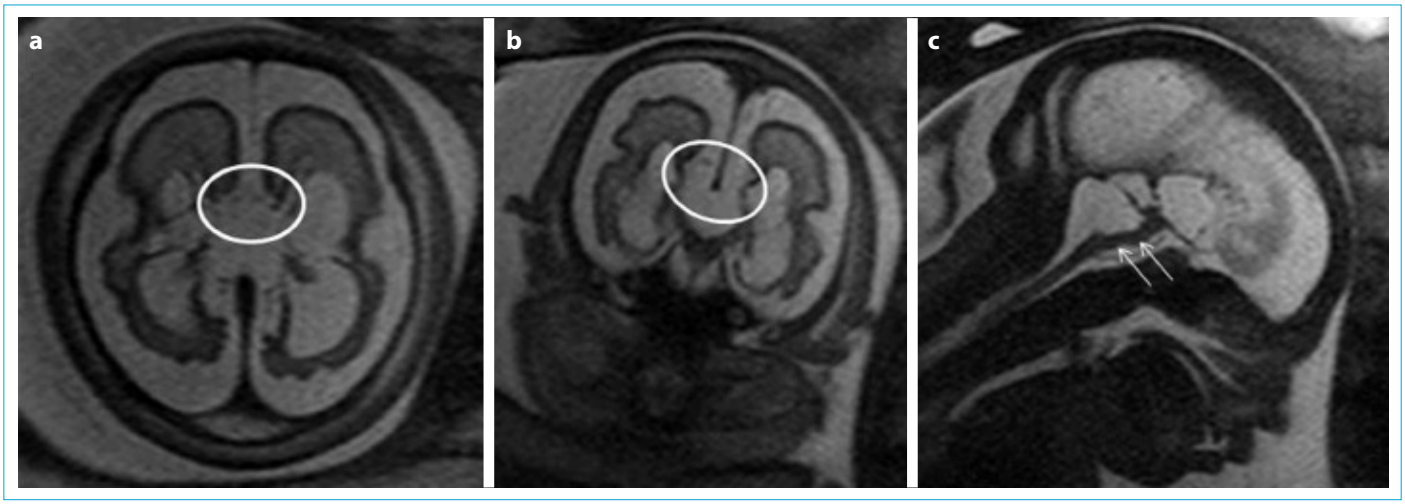

Figure 2 (a-c). Axial **(a)**, coronal **(b)**, and sagittal **(c)** T2-weighted MRI show total corpus callosum agenesis (circle). In addition, cerebellar tissue is not observed. The brainstem is hypoplasic (thin arrows).

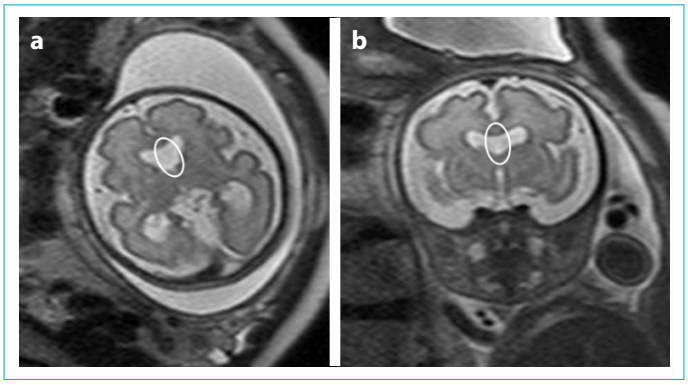

Figure 3 (a, b). Axial **(a)** and coronal **(b)** T2-weighted images show septum pellicidum which separates lateral ventricules is not observed (circle).

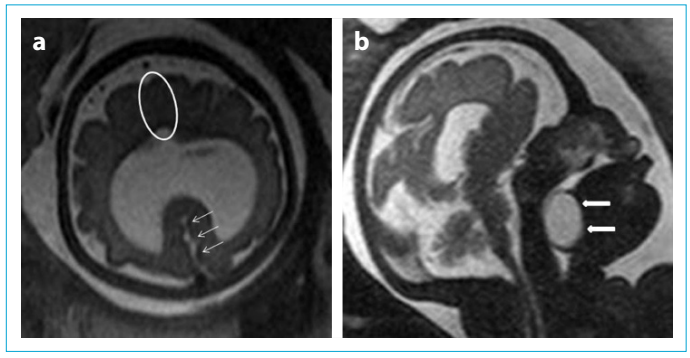

Figure 4 (a, b). (a) Posterior interheminspheric fissure (thin arrows) is seen in T2-weighted axial view, but anterior interheminspheric fissure is not observed (circle) in a fetus with semilobar holoprosencephaly. **(b)** There is a thyroglossal duct cyst at the posterior of the tongue (thick arrows) in T2-weighted sagittal view.

served in 2 of these 6 patients in MRI. In a fetus with cerebral parenchymal injury, intraventricular hemorrhage was additional finding (Fig. 6). Mega cisterna magna and vermis hypoplasia was shown in all cases in MRI (Fig. 7).

Additional MRI findings (n=5, 9%) contributed to patient management (subependymal nodules (n=2), hypoplastic brainstem, pontocerebellar hypoplasia, dysgenetic cerebellum). In accordance with the findings of USG and MRI, 18 pregnancies were terminated at the request of the parents. Additional MRI findings were detected in 6 (33%) of 18 patients. Postnatal 7 MRI examinations were performed. Additional findings were subependymal nodules (n=1), and mega cisterna magna (n=1).

Discussion

Prenatal USG is a highly effective examination technique for the diagnosis of CNS anomalies during the pregnancy [1, 6]. However, nonspecific appearance of some CNS anomalies, inability to see the brain parenchyma near the USG probe, the lack of clear visualisation of some parenchymal anomalies and posterior fossa structures in late gestation weeks in USG limits the examination [4]. Owing to the ossifiation of skull in the 3rd trimester, it is difficult to visualize brain parenchyma with USG as a result of poor penetration of sound waves [1]. Oligohydramnios and inappropriate fetal head position are limiting factors for USG examination [5, 7]. These problems are eliminated by MRI examination [8]. Fetal MRI has been shown to provide changes in diagnosis, patient counseling and management in cases where USG examination is insufficient [4, 5, 7, 9]. In addition, MRI examination has a higher contrast and spatial resolution, making it possible to evaluate the pathologies in detail. Fetal MRI plays an effective role in decisions such as the necessity of intervention, fetal surgery, and postnatal early surgical intervention [5].

In fetal MRI examination, it is possible to view the anatom-

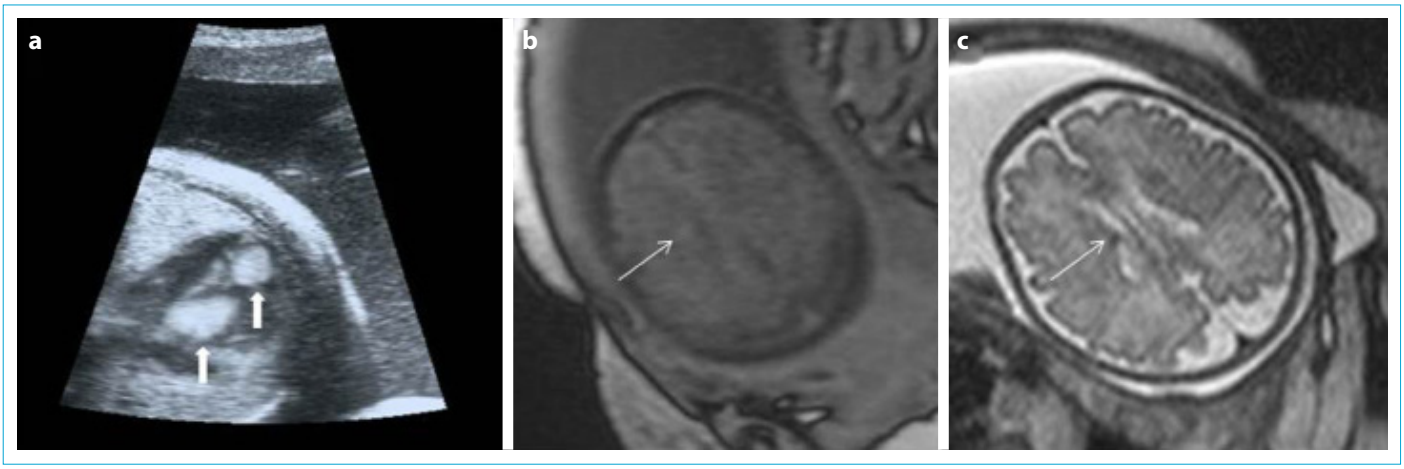

Figure 5 (a-c). (a) Hyperechogenic cardiac rhabdomyomas (thick arrows) are observed in USG examination. **(b, c)** T1 hyperintense and T2 hypointense subependimal nodule is observed in the lateral border of the right lateral ventricle.

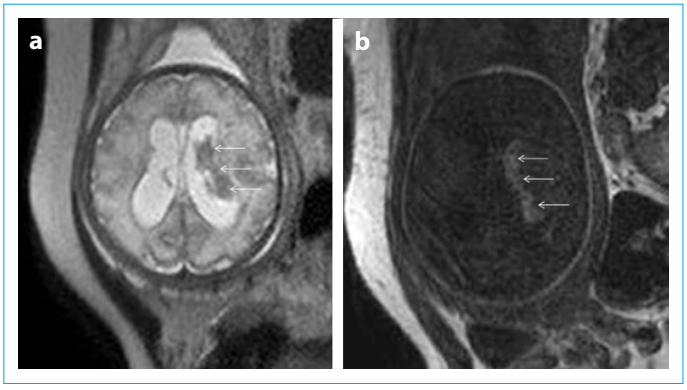

Figure 6 (a, b). Intraventricular hemorrhage (arrows) is seen hypointense in T2-weighted image **(a)**, and hyperintense in T1-weighted image **(b)** in the left lateral ventricule.

ical structures and possible anomalies of the CNS more clearly with T2-weighted images. T1-weighted studies have been reported to be appropriate in patients with suspected bleeding [7]. In some cases, such as tuberous sclerosis, small subependimal nodules or cortical tubers which may not be detected in T2 sequences, may be detected in prenatal and postnatal periods using T1 weighted examination [10]. In our study, axial, sagittal and coronal planes of T2 and axial T1-weighted studies were routinely performed. In cases such as possible bleeding, parenchymal damage and tuberous sclerosis, coronal and sagittal T1 weighted images were added to the routine examination.

The frequency of additional findings after USG is variable in publications and this rate varies between 7-51% [1, 11]. In our study, this rate is 40% which is consistent with literature.

In our study, VM was shown in 26 cases (46%) and is the most common anomaly in accordance with the literature [5, 8, 12]. The causes of VM are diverse and include developmental, destructive and obstructive processes. Hydrocephalus is the endpoint of many pathological processes such as cerebral dysgenesis, cerebral atrophy and encephalomalacia [1]. In patients with VM, additional CNS anomalies were

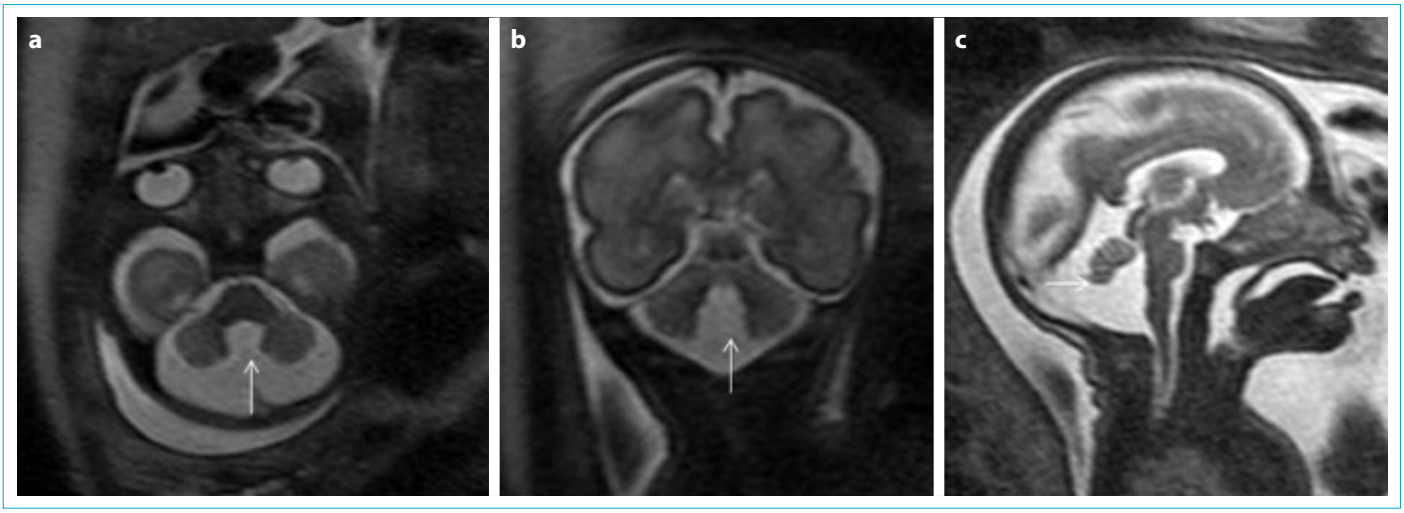

Figure 7 (a-c). Axial **(a)**, coronal **(b)**, and sagittal **(c)** T2-weighted MRI show parsiel vermis hypoplasia (arrow).

found to be 40-50% with fetal MRI [13]. Neural tube defects, CCA, Dandy-Walker complex, lysencephaly, periventricular nodular heterotopia, polymicrogyria, porencephaly, intraventricular and subependimal hemorrhage, and non-CNS chromosomal anomalies may be accompanied VM [8, 12]. In our study, additional findings were shown by MRI in 11 of 26 (42%) patients with VM.

Corpus callosum is one of the 3 major commissors that form the largest connection between the cerebral heminspheres. From the 20th gestational week, the genu of the corpus callosum should be seen [8, 14, 15]. Factors such as the inability to show the midline and the movement of the fetus during the scan may make it difficult to evaluate the corpus callosum in sagittal planes. However, axial and coronal planes are valuable in the evaluation of corpus callosum. Neurodevelopmental disorder incidence increases in the presence of gestational anomalies associated with CCA. It is very important to detect these anomalies because they worsens prognosis [12, 14]. In our study, CCA were shown by USG and MRI in 10 fetuses. In one case, MRI examination showed additional finding of pontocerebellar hypoplasia.

Holoprosencephaly is a malformation spectrum of prosencephalon characterized by a defect in the midline separation of the brain and defect in facial development [16]. Fetal MRI is useful in differentiating holoprosencephaly cases from CCA and midline cysts and clefts [1, 17]. In our study, subgroups of holoprosencephaly were identified by MRI in 2 fetuses.

Tuberous sclerosis (TS) is the most common detected neurocutaneous disease in fetuses. Cardiac rhabdomyoma is the most important clue in the diagnosis of TS. However, half of the fetuses with TS have cardiac rhabdomyoma [18]. Cortical tubers are more common than cardiac rhabdomyomas. Cardiac rhabdomyomas are not commonly seen before the 3rd trimester. For these reasons, performing both USG and MRI may increase prenatal diagnosis of TS [16].

Intracranial hemorrhage may ocur in fetuses with vascular malformation, coagulopathy, trauma or hypoxic-ischemic event [19]. There may be intracranial haemorrhages detected in USG but not seen in MRI. There are also cases where the opposite is reported [20-22]. In our study, intraventricular hemorrhage was detected in 6 cases in USG examination. However, intraventricular hemorrhage was not observed in 2 of these 6 fetuses.

Due to the small size, there are difficulties in the diagnosis of posterior fossa anomalies. Furthermore, the pathological development processes of the cerebellar-vermian and adjacent structures have not been clearly shown. The Dandy Walker variant used in the past is not used by many authors today [23-25]. However, partial vermis agenesis and inferior vermis hypoplasia are used interchangeably by many authors [23, 26, 27]. Discrimination of Blake pouch cyst and arachnoid cyst cannot be made clearly. Postnatal examinations of patients diagnosed with vermis hypoplasia revealed high false positive results. These findings are important examples of the difficulty in diagnosis of anomalies in this region [27]. More accurate results can be reached by the help of studies on the pathological development of the posterior fossa and advances in MRI technique in the future.

In our study, additional findings in 5 fetuses (9%) in MRI examination contributed to patient counseling (subependymal nodule (n=2), DWM, pontocerebellar hypoplasia, infratentorial arachnoid cyst). Parents were informed about prognosis.

In accordance with USG and MRI findings, termination fo pregnancy was performed in 18 cases at the request of the parents. Additional MRI findings were found in 6 (33%) of 18 cases. These additional findings include delayed sulcation (n=2), thinning of the serebral parenchyma (n=2), absence of anterior interheminsferic fissure, thyroglossal duct cyst, polymicrogria, pontocerebellar hypoplasia, subependymal nodule and cortical tuber, cortical dysplasia, and intraventricular hemorrhage.

The main limitation of our study is the lack of pathological diagnosis with autopsy, especially in our country and also all over the world. The reasons for this problem are not having enough pathologist trained in this subject in our country and autopsy is not prefered by parents. In prenatal examination, obstetrics, genetics, child and developmental neurology, radiology, pediatric surgery and pathology should continue to work together. Obstetrics, child-development neurology and radiology team performed our study. The small size of the examined structures and the distance of the examined area to the coils are limitations of the fetal MRI examination. Another limitation of our study is the knowledge of USG findings when MRI scan was performed. To be aware of USG findings provides performing appropriate MRI sequences. Another limitation of our study is only a few postnatal MRI were performed.

In conclusion, the primary examination method for prenatal imaging is USG. Fetal MRI examination is not a substitute for USG examination in anomaly screening. However, MRI is an assistive imaging modality for USG because of the fact that brain structures can be seen more clearly regardless of localization in fetal CNS anomalies by MRI. Considering the findings of our study, we think that fetal MRI will be used more frequently in prenatal diagnosis.

Disclosures

Ethics Committee Approval: The study was approved by the Local Ethics Committee.

Peer-review: Externally peer-reviewed.

Conflict of Interest: None declared.

References

1. Levine D, Barnes PD, Madsen JR, Li W, Edelman RR. Fetal central nervous system anomalies: MR imaging augments sonographic diagnosis. Radiology 1997;204:635–42.
2. Fleischer AC, Manning FA, Jeanty F, Romero R. Sonography in Obstetric and Gynecology, principles and practice. Connecticut, Appleton and Lange 1996;375–93.
3. Tuncel E. Klinik Radyoloji. 2nd. İstanbul: Nobel Tıp Kitabevi; 2011. p. 858–67.
4. Levine D, Barnes PD, Madsen JR, Abbott J, Mehta T, Edelman RR. Central nervous system abnormalities assessed with prenatal magnetic resonance imaging. Obstet Gynecol 1999;94:1011–9.
5. Simon EM, Goldstein RB, Coakley FV, Filly RA, Broderick KC, Musci TJ, et al. Fast MR imaging of fetal CNS anomalies in utero. AJNR Am J Neuroradiol 2000;21:1688–98.
6. Catherine Garel. MRI of the Fetal Brain, Normal Development and Cerebral Pathologies. Secaucus: NJ: Springer-Verlag; 2004. p. 267–621.
7. Wang GB, Shan RQ, Ma YX, Shi H, Chen LG, Liu W, et al. Fetal central nervous system anomalies: comparison of magnetic resonance imaging and ultrasonography for diagnosis. Chin Med J (Engl) 2006;119:1272–7.
8. Glenn OA, Barkovich AJ. Magnetic resonance imaging of the fetal brain and spine: an increasingly important tool in prenatal diagnosis, part 1. AJNR Am J Neuroradiol 2006;27:1604–11.
9. Levine D, Barnes PD, Robertson RR, Wong G, Mehta TS. Fast MR imaging of fetal central nervous system abnormalities. Radiology 2003;229:51–61.
10. Levine D, Barnes P, Korf B, Edelman R. Tuberous sclerosis in the fetus: second-trimester diagnosis of subependymal tubers with ultrafast MR imaging. AJR Am J Roentgenol 2000;175:1067–9.
11. Malinger G, Ben-Sira L, Lev D, Ben-Aroya Z, Kidron D, Lerman-Sagie T. Fetal brain imaging: a comparison between magnetic resonance imaging and dedicated neurosonography. Ultrasound Obstet Gynecol 2004;23:333–40.
12. Levine D, Trop I, Mehta TS, Barnes PD. MR imaging appearance of fetal cerebral ventricular morphology. Radiology 2002;223:652–60.
13. Levine D, Barnes PD, Edelman RR. Obstetric MR imaging. Radiology 1999;211:609–17.
14. Gupta JK, Lilford RJ. Assessment and management of fetal agenesis of the corpus callosum. Prenat Diagn 1995;15:301–12.
15. Kier EL, Truwit CL. The normal and abnormal genu of the corpus callosum: an evolutionary, embryologic, anatomic, and MR analysis. AJNR Am J Neuroradiol 1996;17:1631–41.
16. Levine D, Barnes P. MR imaging of fetal CNS abnor- malities. In: Levine D, editor. Atlas of Fetal MRI. Boca Raton: FL: Taylor & Francis Group; 2005. p. 25–72.
17. Whitby E, Paley MN, Davies N, Sprigg A, Griffiths PD. Ultrafast magnetic resonance imaging of central nervous system abnormalities in utero in the second and third trimester of pregnancy: comparison with ultrasound. BJOG 2001;108:519–26.
18. Bass JL, Breningstall GN, Swaiman KF. Echocardiographic incidence of cardiac rhabdomyoma in tuberous sclerosis. Am J Cardiol 1985;55:1379–82.
19. Fusch C, Ozdoba C, Kuhn P, Dürig P, Remonda L, Müller C, et al. Perinatal ultrasonography and magnetic resonance imaging findings in congenital hydrocephalus associated with fetal intraventricular hemorrhage. Am J Obstet Gynecol 1997;177:512–8.
20. Girard N, Raybaud C, Dercole C, Boubli L, Chau C, Cahen S, et al. In vivo MRI of the fetal brain. Neuroradiology 1993;35:431–6.
21. Canapicchi R, Cioni G, Strigini FA, Abbruzzese A, Bartalena L, Lencioni G. Prenatal diagnosis of periventricular hemorrhage by fetal brain magnetic resonance imaging. Childs Nerv Syst 1998;14:689–92.
22. Fukui K, Morioka T, Nishio S, Mihara F, Nakayama H, Tsukimori K, et al. Fetal germinal matrix and intraventricular haemorrhage diagnosed by MRI. Neuroradiology 2001;43:68–72.
23. Malinger G, Lev D, Lerman-Sagie T. The fetal cerebellum. Pitfalls in diagnosis and management. Prenat Diagn 2009;29:372–80.
24. Guibaud L, des Portes V. Plea for an anatomical approach to abnormalities of the posterior fossa in prenatal diagnosis. Ultrasound Obstet Gynecol 2006;27:477–81.
25. Limperopoulos C, Robertson RL Jr, Khwaja OS, Robson CD, Estroff JA, Barnewolt C, et al. How accurately does current fetal imaging identify posterior fossa anomalies? AJR Am J Roentgenol 2008;190:1637–43.
26. Bolduc ME, Limperopoulos C. Neurodevelopmental outcomes in children with cerebellar malformations: a systematic review. Dev Med Child Neurol 2009;51:256–67.
27. Tilea B, Delezoide AL, Khung-Savatovski S, Guimiot F, Vuillard E, Oury JF, et al. Comparison between magnetic resonance imaging and fetopathology in the evaluation of fetal posterior fossa non-cystic abnormalities. Ultrasound Obstet Gynecol 2007;29:651–9.